Copy
RM E57E03
C2

NACA RM E57E03

NACA

RESEARCH MEMORANDUM

PROPELLANT VAPORIZATION AS A CRITERION FOR ROCKET-ENGINE DESIGN; EXPERIMENTAL EFFECT OF FUEL TEMPERATURE ON LIQUID-OXYGEN - HEPTANE PERFORMANCE

By M. F. Heidmann

Lewis Flight Propulsion Laboratory
Cleveland, Ohio

NATIONAL ADVISORY COMMITTEE FOR AERONAUTICS

WASHINGTON

July 26, 1957

NATIONAL ADVISORY COMMITTEE FOR AERONAUTICS

RESEARCH MEMORANDUM

PROPELLANT VAPORIZATION AS A CRITERION FOR ROCKET-ENGINE DESIGN; EXPERIMENTAL EFFECT OF FUEL TEMPERATURE ON LIQUID-OXYGEN - HEPTANE PERFORMANCE

By M. F. Heidmann

SUMMARY

Characteristic exhaust velocity C^* of a 200-pound-thrust rocket engine was evaluated for fuel temperatures of -90° , 40° , and 200° F with a spray formed by two impinging heptane jets in a highly atomized oxygen atmosphere. Tests covered a range of mixture ratios and chamber lengths.

The C^* efficiency at a mixture ratio of 2.4 (peak theoretical performance) increased from about 60 percent in a 2-inch chamber to 80 percent in an 8-inch chamber; C^* efficiencies were 10 percent higher at a mixture ratio of 1.2. Mixture ratio markedly influenced efficiency, but total propellant flow did not. At nearly all operating conditions and chamber lengths, the C^* efficiency was about 2 percent higher with 200° F heptane than with -90° F heptane. This C^* efficiency increase can be compared with that obtained from a 1/2-inch increase in chamber length. The result agrees with the fuel-temperature effect predicted from an analysis based on droplet-evaporation theory.

INTRODUCTION

Propellant vaporization in rocket-engine combustors is being systematically studied as a criterion for the design of injectors and combustion chambers. Parameters affecting propellant vaporization are investigated analytically, and the results are compared with experimental data from rocket-engine tests.

The importance of the vaporization process has been emphasized in previous studies (refs. 1 to 4). These studies of the effect of injection processes on engine performance showed qualitatively that atomization of the least volatile propellant could control over-all engine performance. Subsequently, numerical calculations were made on the basis that the combustion rate is directly related to the droplet-evaporation rate of the least volatile propellant (ref. 5). Variations

[redacted]

in engine performance caused by changes in drop size, initial propellant temperature, gas velocity, initial drop velocity, combustion temperature, and chamber pressure were computed for heptane droplets in an oxygen atmosphere. Qualitatively, these calculations agree with available data; further substantiation from specific studies of each of these variables under controlled test conditions is required. Initial propellant temperature is one of the first of the variables encountered in the flow path through the combustor. Its effect on engine performance is reported herein.

The characteristic exhaust velocity of a nominal 200-pound-thrust, liquid-oxygen - heptane rocket engine was evaluated for heptane temperatures of -90°, 40°, and 200° F over a range of mixture ratios and chamber lengths. Performance variations with mixture ratio were also studied. These performance tests included mixture variations at a constant fuel-flow rate and fuel-flow-rate variations at a constant mixture. An injector consisting of 2 impinging fuel jets and 24 axial oxidant jets was used. The experimental performance obtained was compared with that computed from the analysis of reference 5.

APPARATUS AND PROCEDURE

Rocket Engine

The rocket engine was designed for a nominal thrust of 200 pounds at a chamber pressure of 300 pounds per square inch. A convergent nozzle with a throat diameter of 0.791 inch and a chamber diameter of 2 inches were used giving a contraction ratio of 6.4. Chamber lengths of 2, 4, 6, and 8 inches were used. The injector, uncooled chambers, and uncooled nozzle were separate units. Spark ignition was used for engine starting. The engine installation was similar to that reported in reference 1.

Propellant Temperature

Three fuel temperatures were studied. Water heated to approximately boiling conditions with an immersion heater produced temperatures of about 200° F; test cell temperatures gave a fuel temperature of 40° F; and a dry ice and alcohol mixture produced a temperature of about -90° F. Temperature regulation at each of these three levels was within approximately ±5° F.

Some of the physical properties of heptane over the temperature range investigated are presented in table I. These data were obtained from reference 6.

Oxygen temperature was maintained constant at -320° F by a liquid-nitrogen bath. The bath extended up to the propellant control valve and included the flow meter and propellant tank.

Injector

The injector used in the study is shown in figure 1. It consisted of two impinging heptane jets, 0.089 inch in diameter, with a 90° impingement angle. The two-dimensional fuel spray was equally spaced between two parallel rows of axial oxidant jets. A total of 24 oxygen jets, 0.0320 inch in diameter, were used. The injector was intended to produce a well defined and reproducible heptane spray in an atmosphere of highly atomized liquid oxygen. Fuel tubes having a large length to diameter ratio were used to insure solid stream impingement, and the point of impingement was extended into the combustor to avoid spray interference with the injector face. Fabrication and operating difficulties limited the size of the oxygen orifices that could be used. A small orifice size was desired so that the oxygen would be highly atomized and would vaporize more rapidly than the fuel.

Performance Measurements

Characteristic-exhaust-velocity measurements were made to evaluate engine performance. Chamber pressure was measured with a direct recording bourdon instrument; occasional pressure comparisons were made with the measurement from a strain-gage pressure transducer. Propellant-flow-rate measurements were made with rotating-vane-type flow meters. Additional flow meters were used in both propellant lines to check the stability of the flow meter calibrations. These additional meters consisted of a rotating-vane-type meter in the fuel line and a venturi meter in the oxidant line. The density of each propellant was evaluated using temperature measurements at the flow meters. Instrument calibrations indicated an accuracy within ±2 percent for C^* measurements. Reproducibility of data was generally within ±1 percent.

The C^* measurements are reported as a percentage of the theoretical performance at the operating mixture ratio (C^* efficiency). Theoretical equilibrium performance and composition for heptane and oxygen at 300 pounds per square inch of chamber pressure are shown in figure 2. Corrections for chamber pressure by the method described in reference 7 were used when corrections exceeded 1/2 percent. The fuel-temperature range investigated affects theoretical C^* by about 1/4 percent. This effect was neglected in the reported data.

Procedure

Engine firings were made with heptane at temperatures of 200°, 40°, and -90° F. C^* efficiency was measured for chamber lengths of 2, 4, 6, and 8 inches and mixture ratios of 1.2 to 4.0 (20 to 45 percent fuel). For most tests, a constant total-propellant flow rate of about 0.9 pound per second was used. Test firings were about 3 seconds in duration.

Several firings were made with various total-propellant flow rates in order to study the effect of changes in fuel-spray characteristics on C^* efficiency. 4531

RESULTS AND DISCUSSION

Experimental Fuel-Temperature Effect

The C^* efficiency obtained at constant total-flow-rate conditions for all chamber lengths and fuel temperatures is shown as a function of oxidant-fuel mixture in figure 3. These data are also presented in table II. In general, the C^* efficiency increased from about 60 percent in a 2-inch chamber to 80 percent in an 8-inch chamber. The effect of mixture ratio was small between stoichiometric and peak theoretical conditions; however, at more fuel-rich conditions, an increase in efficiency was obtained.

The effect of fuel temperature on C^* efficiency was relatively small. An increase in efficiency with an increase in temperature, however, was generally observed. Faired curves through the upper and lower limits of the data in figure 3 show an increase in efficiency of approximately 2 percent for the 290° F increase in fuel temperature. Typical data scatter prevents resolving any effect less than about 2 percent in performance.

Computed Fuel-Temperature Effect

Figure 4 shows the calculated effect of initial heptane temperature on droplet evaporation reported in reference 5. The percent-fuel evaporated is shown as a function of chamber length for initial temperatures of -60°, 40°, and 240° F. Conditions were assumed approximately close to those used in the experimental tests except that calculations were for a single size drop. The fuel spray used produced a distribution of drop sizes which probably included drops considerably larger than that size assumed in the analysis.

The correlation of experimental and theoretical results depends to some degree on a knowledge of drop history within the chamber. It has been shown in reference 5 that the temperature of a fuel drop increases from its initial temperature to an equilibrium temperature of about 390° F for the condition being studied. Vaporization rate during this transient period is extremely low. The increment of chamber length required for this transient condition should vary with initial fuel temperature. Laterally shifting the percent evaporated against chamber-length curves is suggested as a method of correlating fuel temperature. Such a correlation of the theoretical data is shown in figure 5, using the 40° F curve as a reference and the correlation point at 60-percent fuel evaporated. The lateral displacement of the curves is such that a temperature increase of 100° F produces the same effect on C^* efficiency as a chamber-length increase of 0.14 inch.

Comparison of Experimental and Computed Fuel-Temperature Effect

The experimental data in figure 6 are compared with the theoretical curves in figure 4. The variation in C^* efficiency with chamber length is shown for 200°, 40°, and -90° F. An arithmetic average of the performance data between mixture ratios of 20 to 30 percent fuel by weight was used. The increase in efficiency with an increase in chamber length is similar to that calculated on the basis of droplet evaporation; however, complete evaporation was predicted in a much shorter chamber length than that indicated by the C^* efficiency values. In discussing such comparisons in reference 5, the difference was attributed to the effect of a drop-size distribution on vaporization rates. Although such differences exist, the calculated effect of fuel temperature on evaporation, expressed in terms of an equivalent chamber-length change, should be approximately correct.

The experimental data, corrected for the calculated effect of a fuel temperature change, are shown in figure 7. A single-curve correlation within experimental accuracy is obtained. The 290° F increase in fuel temperature produces an increase in C^* efficiency of about the same magnitude as that obtained from a 1/2-inch increase in chamber length.

Fuel-Spray and Mixture-Ratio Effects

The increase in C^* efficiency with fuel temperature obtained experimentally may result from a change in the vaporization rate with initial fuel temperature as well as from changes in spray characteristics with fuel temperature. Spray changes may be incurred because injection velocity, injection momentum, liquid viscosity, and surface tension will vary with fuel-temperature changes. The significance of these spray changes is not known directly. Changes in fuel injection velocity and momentum are also incurred during a variation in mixture ratio. The variations of efficiency with mixture ratio were studied more fully to resolve these jet velocity and momentum effects.

Several tests were made to isolate the cause of changes in C^* efficiency with mixture ratio. In figure 8(a) the effect of mixture ratio on performance is shown for (1) constant fuel flow - variable total flow and (2) variable fuel flow - constant total flow. The variation in performance is similar for both conditions even though fuel-spray characteristics could vary for one condition and not for the other. The performance difference for the two conditions could have been less if chamber pressure had not by necessity varied for the variable total-flow tests. An increase in pressure should accelerate the vaporization process as reported in reference 5 and, qualitatively, this effect would improve agreement. 4531
The importance of spray changes due to injection velocity and momentum, therefore, appear to be small in the case considered herein.

Similar conclusions may be drawn from the comparison shown in figure 8(b). The effect of fuel-flow rate on performance is shown for the following two conditions: (1) constant mixture - variable total flow and (2) variable mixture - constant total flow. Variations in performance with the fuel flow rate are small when the mixture ratio is maintained constant. The small increase that does occur in C^* efficiency with the flow rate may again result from chamber-pressure variations caused by changes in total flow.

On the basis of these tests, it was concluded that C^* efficiency is primarily dependent on the proportions of oxidant and fuel used and relatively independent of spray changes which may have been incurred by mixture-ratio or fuel-temperature changes.

CONCLUDING REMARKS

The correlation of the experimental and theoretical effect of fuel temperature on engine performance confirms, in part, that calculations based on droplet-evaporation theory can be used to predict variations in engine performance. The importance of droplet evaporation in the over-all combustion process and the validity of the assumptions used in the calculations, however, require further verification. The need for experimental studies on the effect of drop size, chamber pressure, gas velocity, and other parameters on engine performance is indicated.

A larger effect of fuel temperature on performance may be expected if the change in temperature significantly affects the spray characteristics. When the fuel is heated to the point where vapor or vapor-liquid mixtures are injected, spray and performance changes would undoubtedly result. The degree of jet ruffling and orifice cavitation may also be sensitive to fuel temperature in some instances. Such conditions would tend to exaggerate the effect of fuel temperature on performance.

The small effect of fuel temperature obtained with heptane may not apply directly to other fuels. Further studies, both theoretical and experimental, would be required in order to generalize the effect of temperature with respect to fuel type.

The effect of mixture ratio on C^* efficiency, observed in these studies, requires further verification at higher efficiency levels and with other injection methods before such an effect can be generalized. Efficiency variations with mixture ratio are important to rocket combus-
4551 tion technology for they may indicate changes in chemical kinetic, mixing, and vaporization processes.

SUMMARY OF RESULTS

Characteristic exhaust velocity of a 200-pound liquid-oxygen - heptane rocket engine was experimentally evaluated for heptane temperatures of -90°, 40°, and 200° F over a range of mixture ratios and chamber lengths, and for a spray formed by two impinging heptane jets in a highly atomized liquid-oxygen atmosphere. At a mixture ratio of 2.4 (peak theoretical performance), the injectors gave C^* efficiencies of about 60 percent in a 2-inch chamber and 80 percent in an 8-inch chamber; C^* efficiencies were 10 percent higher at a mixture ratio of 1.2. The results obtained are summarized as follows:

1. Efficiency varied markedly with the proportions of oxidant and fuel rather than with total propellant flow or fuel temperature, which implies that mixture composition was a more important factor in combustion than gross spray characteristics.

2. Characteristic velocity was approximately 2 percentage points higher with 200° F fuel than with -90° F fuel. The performance increase can be compared with that obtained by increasing chamber length by about 1/2 inch.

3. The results agree with the temperature effect predicted from calculations based on droplet-evaporation theory; theoretically, the performance increase resulting from a 100° F increase in fuel temperature should equal that obtained from a 0.14-inch increase in chamber length.

Lewis Flight Propulsion Laboratory
National Advisory Committee for Aeronautics
Cleveland, Ohio, May 3, 1957

REFERENCES

1. Heidmann, M. F., and Auble, C. M.: Injection Principles from Combustion Studies in a 200-Pound-Thrust Rocket Engine Using Liquid Oxygen and Heptane. NACA RM E55C22, 1955.

2. Heidmann, M. F.: A Study of Injection Processes for 15-Percent Fluorine - 85-Percent Oxygen and Heptane in a 200-Pound-Thrust Rocket Engine. NACA RM E56J11, 1957.

3. Auble, Carmon M.: A Study of Injection Processes for Liquid Oxygen and Gaseous Hydrogen in a 200-Pound-Thrust Rocket Engine. NACA RM E56I25a, 1956.

4. Heidmann, Marcus F.: Injection Principles for Liquid Oxygen and Heptane Using Two-Element Injectors. NACA RM E56D04, 1956.

5. Priem, Richard J.: Propellant Vaporization as a Criterion for Rocket Design; Numerical Calculations of Chamber Length to Vaporize a Single Hydrocarbon Drop. NACA TN 3985, 1957.

6. Rossini, Frederick D., et al.: Selected Values of Physical and Thermodynamic Properties of Hydrocarbons and Related Compounds. Carnegie Press (Pittsburgh), 1953.

7. Huff, Vearl N., Fortini, Anthony, and Gordon, Sanford: Theoretical Performance of JP-4 Fuel and Liquid Oxygen as a Rocket Propellant. II - Equilibrium Composition. NACA RM E56D23, 1956.

4531

CR-2

TABLE I. - PROPERTIES OF n-HEPTANE

[Data obtained from ref. 6.]

Chemical formula		C_7H_{16}
Molecular weight		100
Normal boiling point, °F		209
Freezing point, °F		-131
Heat of vaporization, Btu/lb		
77° F		157
209° F		136
Heat of combustion, Btu/lb		
Gaseous n-heptane	$H_2O_{liq}CO_{2gas}$	20825
	$H_2O_{gas}CO_{2gas}$	19314
Liquid n-heptane	$H_2O_{liq}CO_{2gas}$	20668
	$H_2O_{gas}CO_{2gas}$	19157

Temperature, °F	Viscosity abs, centipoises	Surface tension, dynes/cm	Density, lb/cu ft	Heat content, Btu/lb
-459.7	-----	----	-----	0
-90	1.82	----	47.21	------
-60	1.21	----	46.38	------
-30	.878	25.7	45.53	------
0	.671	24.1	44.67	105.52
30	.534	22.4	43.79	115.7
60	.442	20.8	42.92	126.55
90	.370	19.8	42.04	138.0
120	.316	17.5	41.16	------
150	.274	15.9	40.20	------
180	.229	13.8	39.22	------
210	.210	----	38.21	188

4531

TABLE II. - ENGINE PERFORMANCE DATA

(a) Heptane temperature, -90° F.

Run	Chamber pressure, lb/sq in. abs	Oxidant-flow meter			Fuel-flow meter			Oxidant flow, lb/sec	Fuel flow, lb/sec	Total flow, lb/sec	Mixture ratio		Characteristic velocity		
		cps_1	Venturi, ΔP	$\frac{cps_1}{\sqrt{\Delta P}}$	cps_1	cps_2	$\frac{cps_2}{cps_1}$				Percent fuel	Oxidant fuel	Experimental, ft/sec	Theoretical, ft/sec	Experimental percent of theory
Chamber length, 2 in.															
721	209	228	42.4	35.1	63.3	210	3.32	0.582	0.324	0.906	35.7	1.80	3640	5750	63.2
722	198	273	60.6	35.1	41.4	136	3.29	.696	.212	.908	23.4	3.28	3450	5700	60.6
723	205	206	34.9	34.9	73.8	247	3.35	.526	.377	.903	41.7	1.39	3590	5160	69.5
724	208	250	51.0	35.0	51.2	169	3.30	.638	.262	.900	29.1	2.44	3650	5930	61.5
Chamber length, 4 in.															
725	235	228	42.0	35.2	63.3	211	3.34	0.582	0.323	0.905	35.7	1.80	4100	5750	71.3
726	220	283	65.0	35.2	36.3	117	3.23	.722	.186	.908	20.5	3.88	3830	5500	69.6
727	234	211	36.0	35.2	73.5	246	3.35	.538	.376	.914	41.1	1.43	4050	5220	77.5
728	238	253	53.3	34.7	51.6	170	3.29	.645	.264	.909	29.0	2.44	4140	5930	69.8
Chamber length, 6 in.															
729	249	232	44.2	35.0	59.8	202	3.38	0.592	0.305	0.897	34.0	1.94	4390	5850	75.0
730	240	278	66.5	34.1	38.0	123	3.24	.709	.194	.903	21.5	3.65	4200	5580	75.3
731	243	208	35.5	34.9	72.8	244	3.35	.530	.372	.902	41.2	1.42	4250	5210	81.5
732	248	255	53.0	35.1	47.8	160	3.35	.650	.244	.894	27.3	2.66	4390	5880	74.6
Chamber length, 8 in.															
733	262	232	44.2	34.9	59.3	199	3.36	0.591	0.303	0.894	33.9	1.95	4630	5850	79.2
734	247	277	62.6	35.0	36.9	118	3.20	.707	.188	.895	21.0	3.76	4360	5540	78.8
735	252	208	35.4	35.0	70.7	238	3.37	.530	.362	.892	40.5	1.46	4460	5270	84.5
736	266	254	53.3	34.8	51.0	168	3.30	.648	.261	.909	28.7	2.48	4630	5920	78.2
Constant fuel flow; variable mixture; chamber length, 4 in.															
737	134	103	-----	----	58.1	193	3.32	0.263	0.297	0.560	53.0	0.885	3780	[a]4290	88.1
738	188	177	25.7	35.0	59.0	195	3.31	.452	.301	.753	40.0	1.50	3940	[a]5340	73.8
739	258	297	72.0	35.1	50.3	165	3.28	.757	.257	1.014	25.3	2.94	4020	[a]5800	69.3
740	299	366	-----	----	50.5	167	3.31	.934	.258	1.192	21.6	3.62	3960	[a]5590	71.0
Variable fuel flow; constant mixture; chamber length, 4 in.															
741	147	172	24.0	35.1	31.4	101	3.22	0.438	0.161	0.599	26.9	2.72	3890	[a]5810	66.9
742	194	211	36.7	34.9	44.0	140	3.18	.538	.225	.763	29.5	2.39	4030	[a]5910	68.2
743	272	287	67.5	35.0	59.3	197	3.32	.732	.303	1.035	29.3	2.42	4150	[a]5935	70.0
744	34[illegible]	352	-----	----	73.5	245	3.34	.898	.375	1.273	29.4	2.39	4250	[a]5950	71.4

[a] Corrected for chamber pressure.

TABLE II. - Continued. ENGINE PERFORMANCE DATA

(b) Heptane temperature, 40° F.

Run	Chamber pressure, lb/sq in. abs	Oxidant-flow meter			Fuel-flow meter			Oxidant flow, lb/sec	Fuel flow, lb/sec	Total flow, lb/sec	Mixture ratio		Characteristic velocity		
		cps_1	Venturi, ΔP	$\frac{cps_1}{\sqrt{\Delta P}}$	cps_1	cps_2	$\frac{cps_2}{cps_1}$				Percent fuel	Oxidant fuel	Experimental, ft/sec	Theoretical, ft/sec	Experimental percent of theory
Chamber length, 2 in.															
716	213	235	44.1	35.4	67.4	228	3.39	0.600	0.316	0.916	34.5	1.90	3680	5820	63.2
717	195	265	56.6	35.2	42.1	142	3.38	.676	.198	.874	22.6	3.41	3530	5660	62.3
718	205	206	34.1	35.3	81.7	277	3.39	.525	.383	.908	42.2	1.37	3570	5130	69.5
719	207	252	51.2	35.2	55.5	188	3.39	.643	.261	.904	28.9	2.46	3620	5930	61.0
720	208	272	59.8	35.2	47.9	162	3.38	.694	.224	.918	24.4	3.10	3580	5760	62.0
Chamber length, 4 in.															
659	253	265	56.3	35.3	61.0	205	3.36	0.675	0.283	0.958	29.5	2.38	4170	5940	70.3
660	238	250	50.3	34.8	59.8	198	3.31	.638	.273	.911	29.9	2.34	4130	5940	69.6
661	227	268	57.5	35.3	48.2	161	3.34	.683	.222	.905	24.5	3.08	3960	5760	68.7
662	234	225	40.8	35.2	70.9	239	3.37	.574	.330	.904	36.5	1.74	4100	5690	72.1
663	225	290	67.7	35.3	42.0	140	3.38	.740	.193	.933	20.7	3.84	3820	5500	69.5
664	232	196	30.5	35.5	90.2	304	3.38	.500	.420	.920	45.6	1.19	3990	4820	82.7
Chamber length, 6 in.															
712	252	231	43.0	35.3	67.8	229	3.38	0.590	0.318	0.908	35.0	1.85	4390	5790	75.8
713	241	275	60.5	35.4	41.8	141	3.37	.702	.196	.898	21.8	3.58	4250	5600	76.0
714	242	208	34.6	35.4	80.0	271	3.38	.530	.375	.905	41.5	1.41	4230	5210	81.0
715	255	252	51.2	35.2	56.7	192	3.38	.643	.266	.909	29.3	2.42	4440	5940	74.7
Chamber length 8, in.															
708	258	226	40.9	35.4	66.7	226	3.39	0.576	0.313	0.889	35.2	1.84	4590	5780	79.3
709	254	276	60.7	35.5	41.8	142	3.40	.705	.196	.901	21.8	3.60	4450	5600	79.5
710	251	206	33.5	35.6	79.6	270	3.39	.525	.374	.899	41.6	1.40	4420	5170	85.5
711	266	251	49.8	35.6	56.5	191	3.38	.640	.265	.905	29.3	2.41	4650	5940	78.3
Constant fuel flow; variable mixture; chamber length, 4 in.															
745	133	110.5	10.2	35.1	59.8	---	----	0.282	0.283	0.565	50.0	0.995	3720	[a]4490	82.9
746	189	185	28.2	34.9	58.7	201	3.43	.472	.278	.750	37.0	1.70	3980	[a]5640	70.7
747	261	293	70.5	35.0	54.5	184.5	3.39	.748	.258	1.006	25.7	2.90	4100	[a]5820	70.5
748	295	373	112	35.2	49.6	169.5	3.42	.951	.235	1.186	19.8	4.05	3930	[a]5460	71.9
Variable fuel flow; constant mixture; chamber length, 4 in.															
749	137	169	23.4	34.9	31.3	105	3.36	0.430	0.148	0.578	25.6	2.90	3750	[a]5750	65.3
750	193	208	35.7	34.9	47.5	159	3.35	.530	.224	.754	29.7	2.36	4050	[a]5900	68.7
751	275	285	66.1	35.0	66.6	228	3.42	.728	.315	1.043	30.2	2.31	4160	[a]5940	70.2
752	345	357	102.8	34.8	78.0	---	----	.910	.369	1.279	28.9	2.46	4270	[a]5930	72.1

[a]Corrected for chamber pressure.

TABLE II. - Concluded. ENGINE PERFORMANCE DATA

(c) Heptane temperature, 200° F.

Run	Chamber pressure, lb/sq in. abs	Oxidant-flow meter			Fuel-flow meter			Oxidant flow, lb/sec	Fuel flow, lb/sec	Total flow, lb/sec	Mixture ratio		Characteristic velocity		
		cps_1	Venturi, ΔP	$\frac{cps_1}{\sqrt{\Delta P}}$	cps_1	cps_2	$\frac{cps_2}{cps_1}$				Percent fuel	Oxidant fuel	Experimental, ft/sec	Theoretical, ft/sec	Experimental percent of theory
Chamber length, 2 in.															
691	216	214	36.7	35.3	88.0	298	3.38	0.546	0.370	0.916	40.8	1.48	3730	5300	70.3
692	215	235	44.2	35.3	75.0	252	3.37	.600	.312	.913	34.5	1.92	3730	5840	63.9
694	210	252	51.5	35.1	84.0	215	3.36	.643	.266	.909	29.3	2.42	3660	5930	61.7
695	198	255	51.5	35.6	54.7	185	3.38	.651	.229	.880	26.0	2.84	3560	5830	61.1
Chamber length, 4 in.															
686	254	316	80.1	35.3	49.0	166	3.39	0.806	0.206	1.012	20.5	3.92	3970	5480	72.4
687	244	218	38.8	35.0	89.0	299	3.36	.556	.371	.927	40.2	1.50	4160	5340	78.0
688	243	230	43.6	34.9	78.5	265	3.38	.587	.329	.916	36.4	1.78	4200	5730	73.3
689	247	245	48.8	35.1	68.0	229	3.37	.625	.284	.909	31.3	2.20	4300	5940	72.4
690	242	277	61.4	35.3	54.5	182	3.34	.707	.226	.933	24.4	3.12	4100	5750	71.3
Chamber length, 6 in.															
697	253	210	36.3	34.9	86.0	287	3.34	0.536	0.356	0.892	39.9	1.51	4480	5350	82.0
698	259	245	48.8	35.1	68.2	230	3.37	.625	.285	.910	31.3	2.20	4500	5940	75.8
699	262	257	53.5	35.2	62.5	210	3.36	.655	.260	.915	28.4	2.52	4520	5920	76.3
700	252	236	45.0	35.2	69.5	---	----	.602	.291	.893	32.6	2.07	4470	5910	75.7
701	233	236	44.6	35.3	54.2	---	----	.602	.226	.828	27.3	2.66	4450	5880	75.8
702	254	280	62.6	35.4	50.5	---	----	.715	.211	.926	22.8	3.39	4340	5660	76.5
Chamber length, 8 in.															
703	271	249	49.8	35.3	63.7	---	----	0.635	0.267	0.920	29.6	2.38	4750	5940	80.0
704	258	213	36.0	35.5	83.0	---	----	.543	.347	.890	39.0	1.56	4600	5430	84.7
706	263	231	42.8	35.4	72.2	---	----	.589	.302	.891	33.9	1.95	4670	5850	80.0
707	272	267	54.5	36.2	57.5	---	----	.682	.240	.922	26.0	2.84	4660	5830	80.0

4531

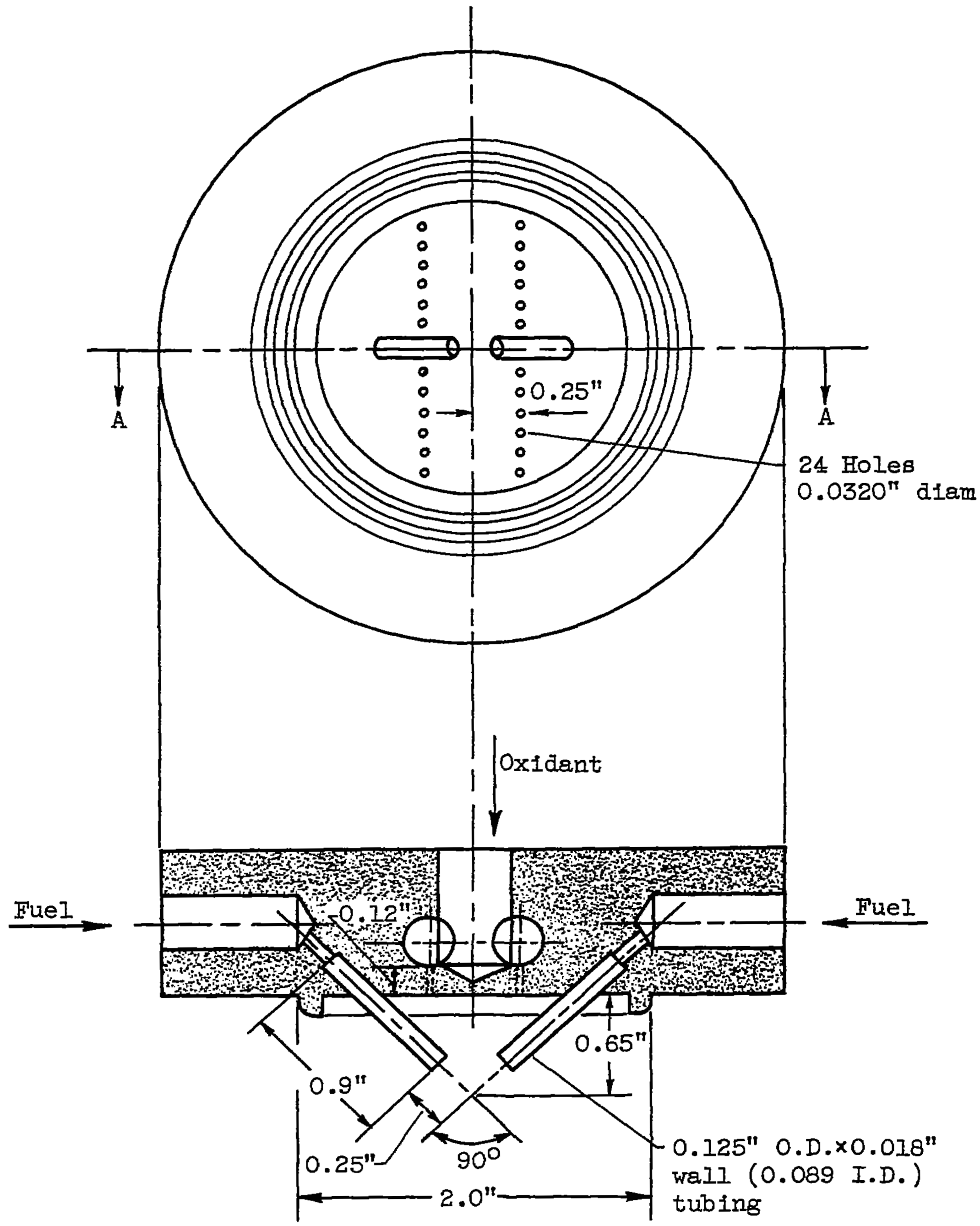

Section AA

Figure 1. - Injector design simulating impinging-jet fuel spray in a highly atomized oxidant atmosphere.

4531

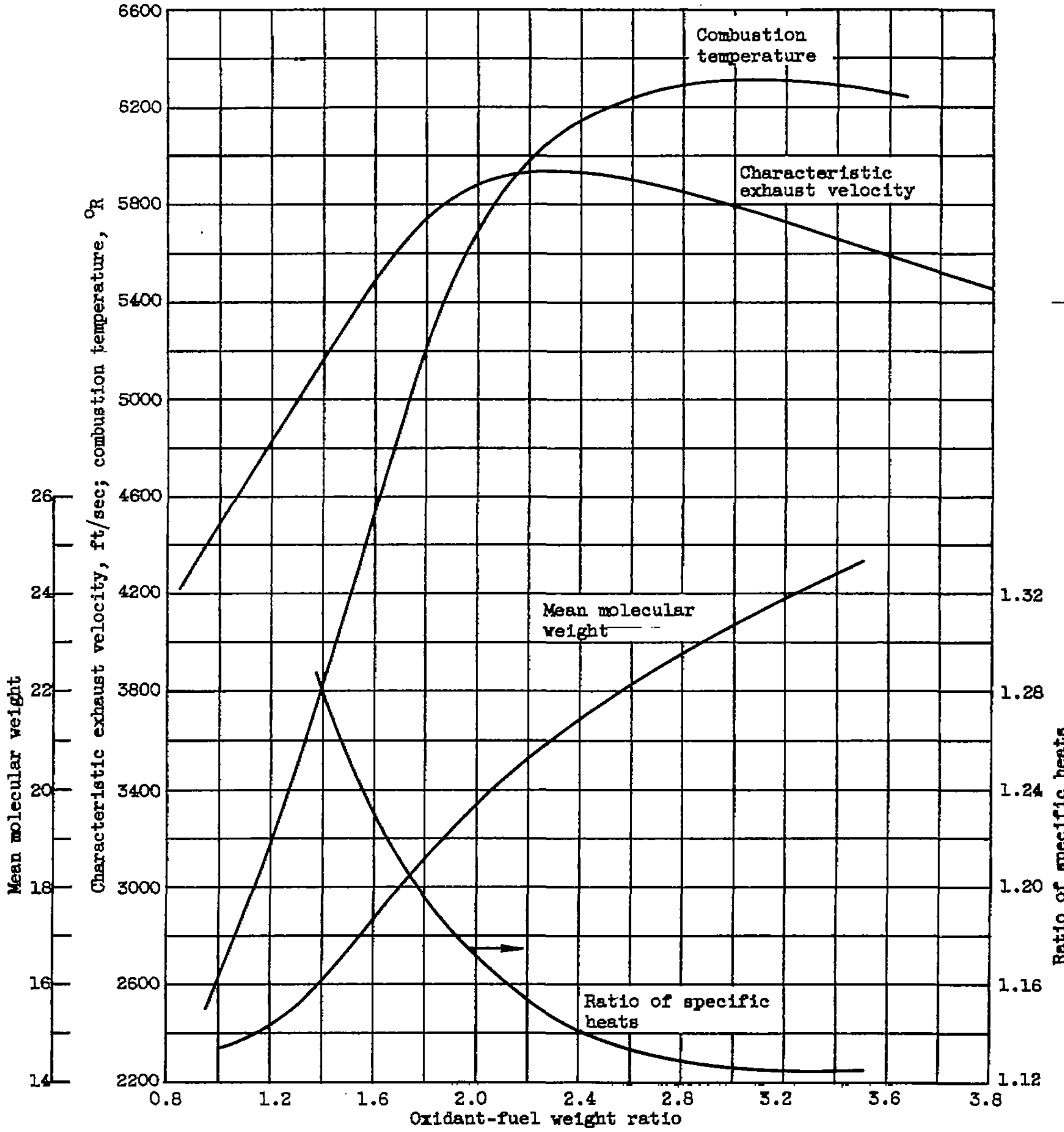

Figure 2. - Theoretical equilibrium combustion properties of heptane - oxygen propellant combination at 300 pounds per square inch.

4531

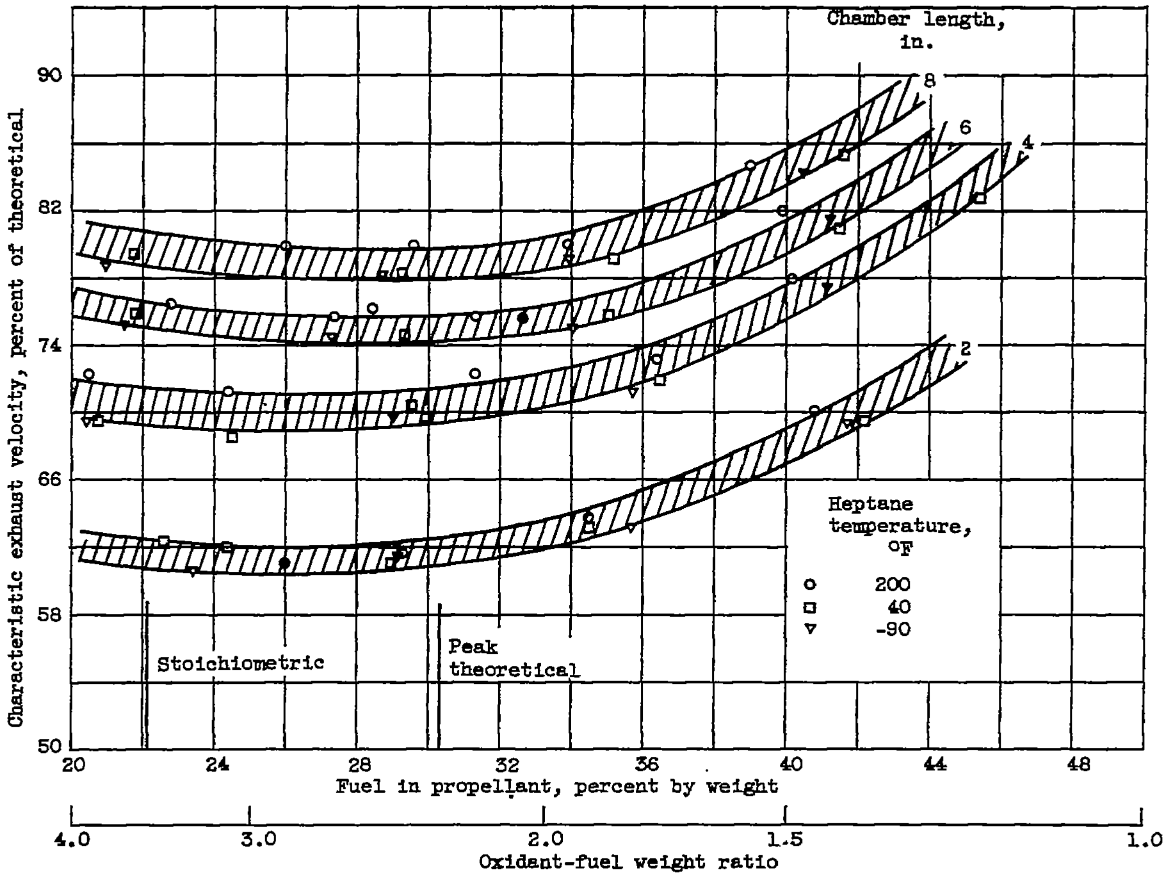

Figure 3. - Effect of initial fuel temperature on characteristic exhaust velocity.

[redacted]

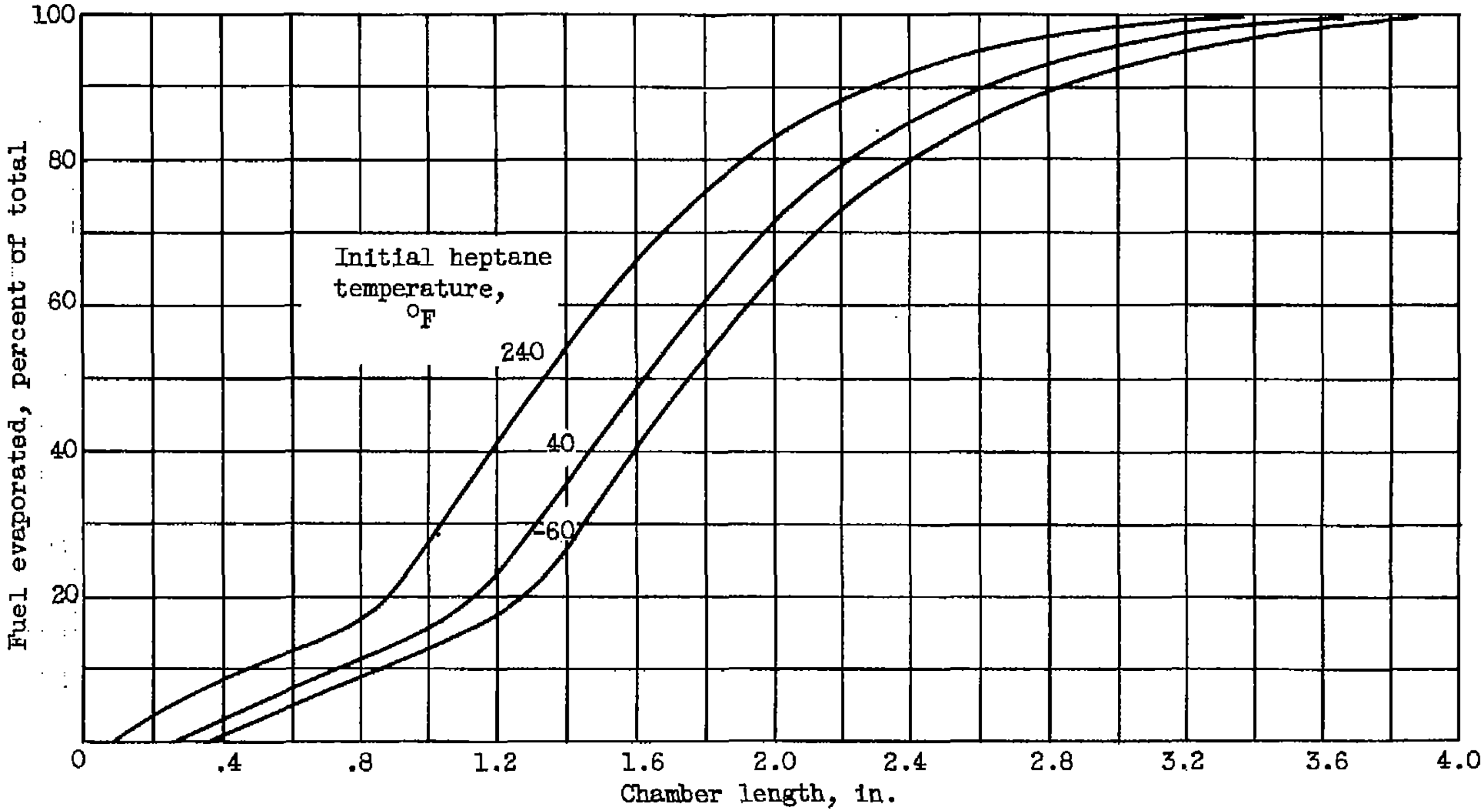

Figure 4. - Calculated effect of initial heptane temperature on fuel evaporated as a function of chamber length. Assumed conditions: Drop diameter, 0.006 inch; initial drop velocity, 100 feet per second; chamber pressure, 300 pounds per square inch absolute; final gas velocity, 800 feet per second (ref. 5).

[redacted]

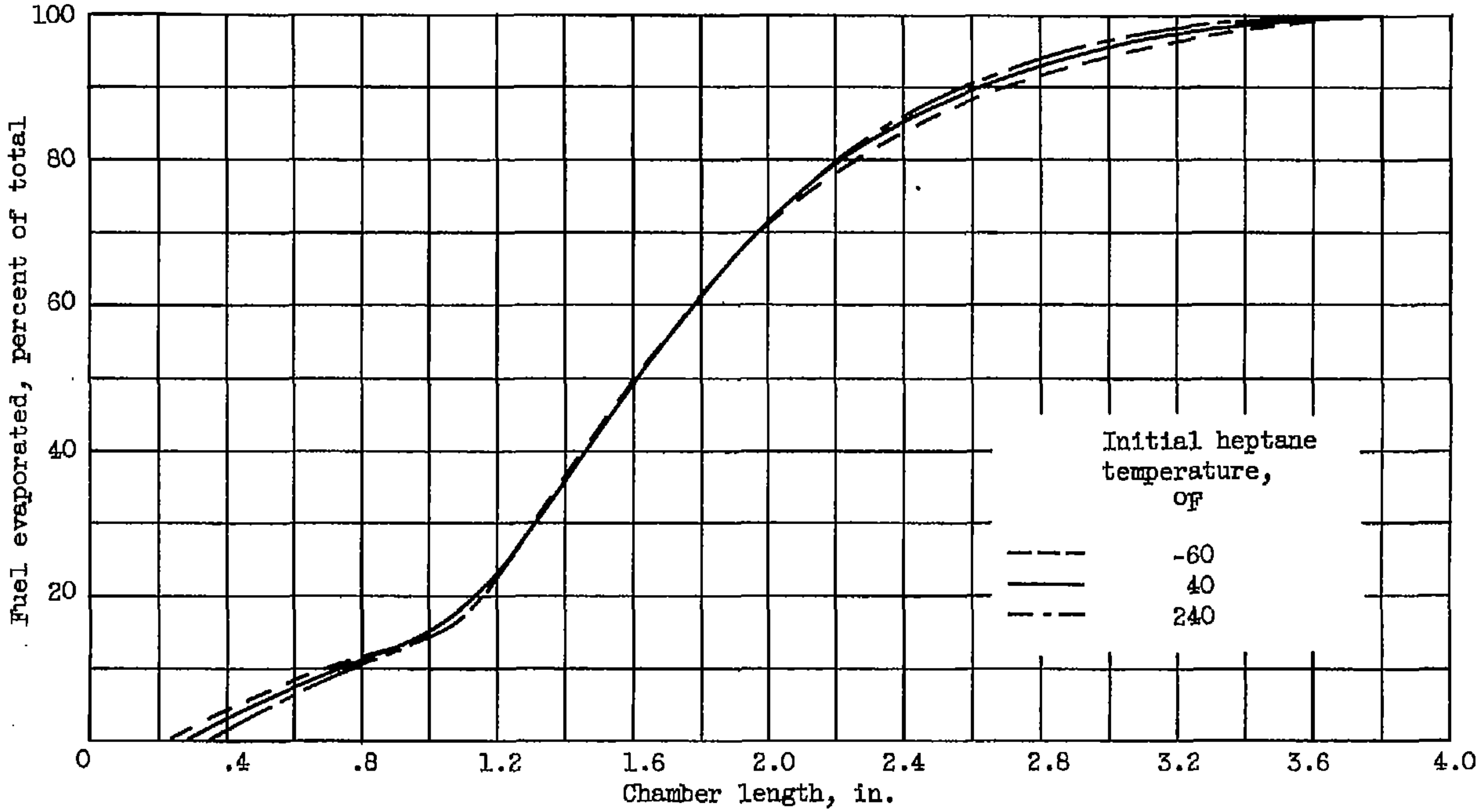

[redacted]

Figure 5. - Correlation of calculated data assuming equal increases in fuel evaporated from a 100° F increase in fuel temperature and a 0.14-inch increase in chamber length. Reference curve is 40° F curve of figure 4.

[redacted]

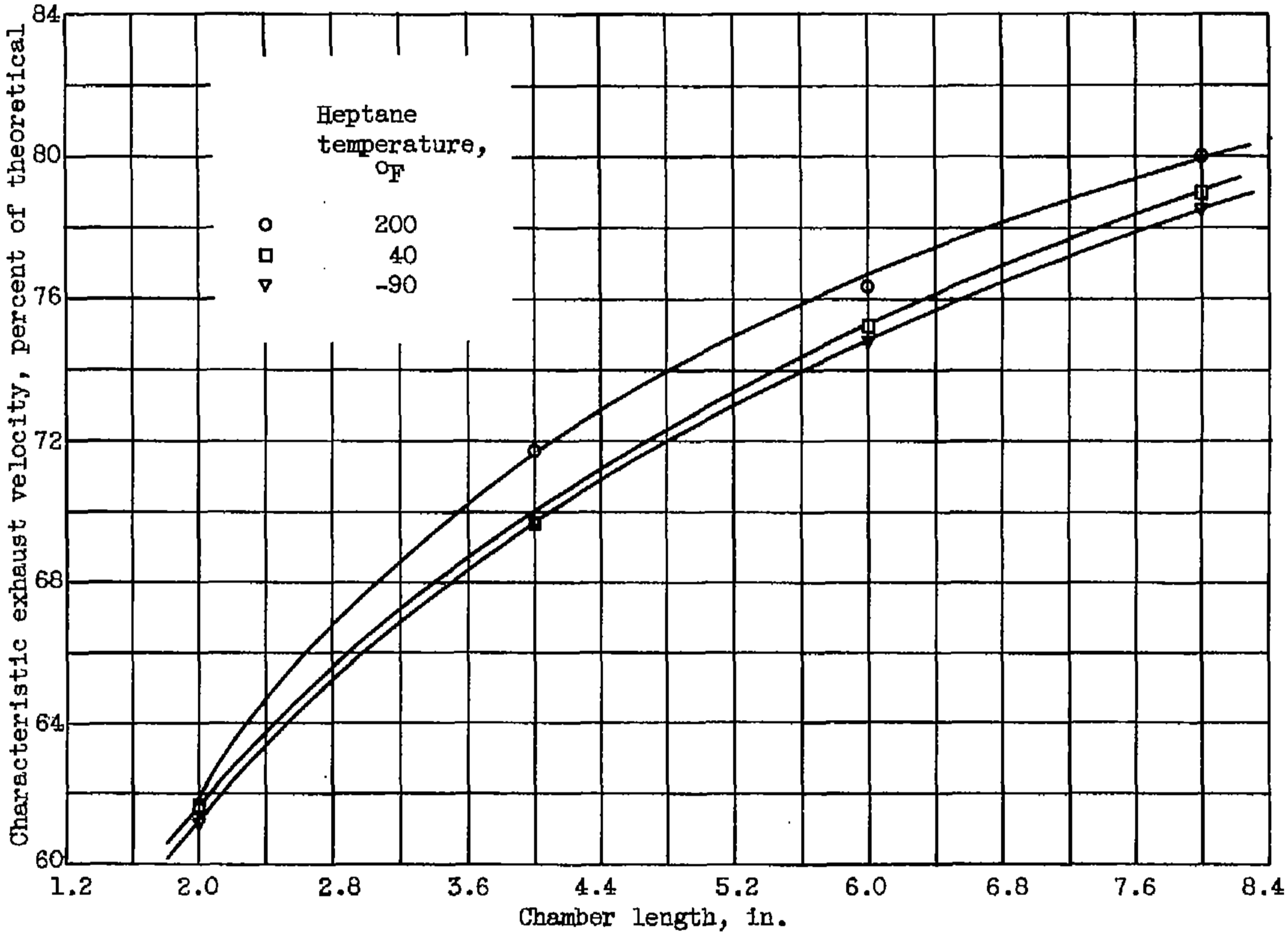

Figure 6. - Experimental effect of heptane temperature on performance as a function of chamber length. Average performance between stoichiometric and peak theoretical mixtures.

[redacted]

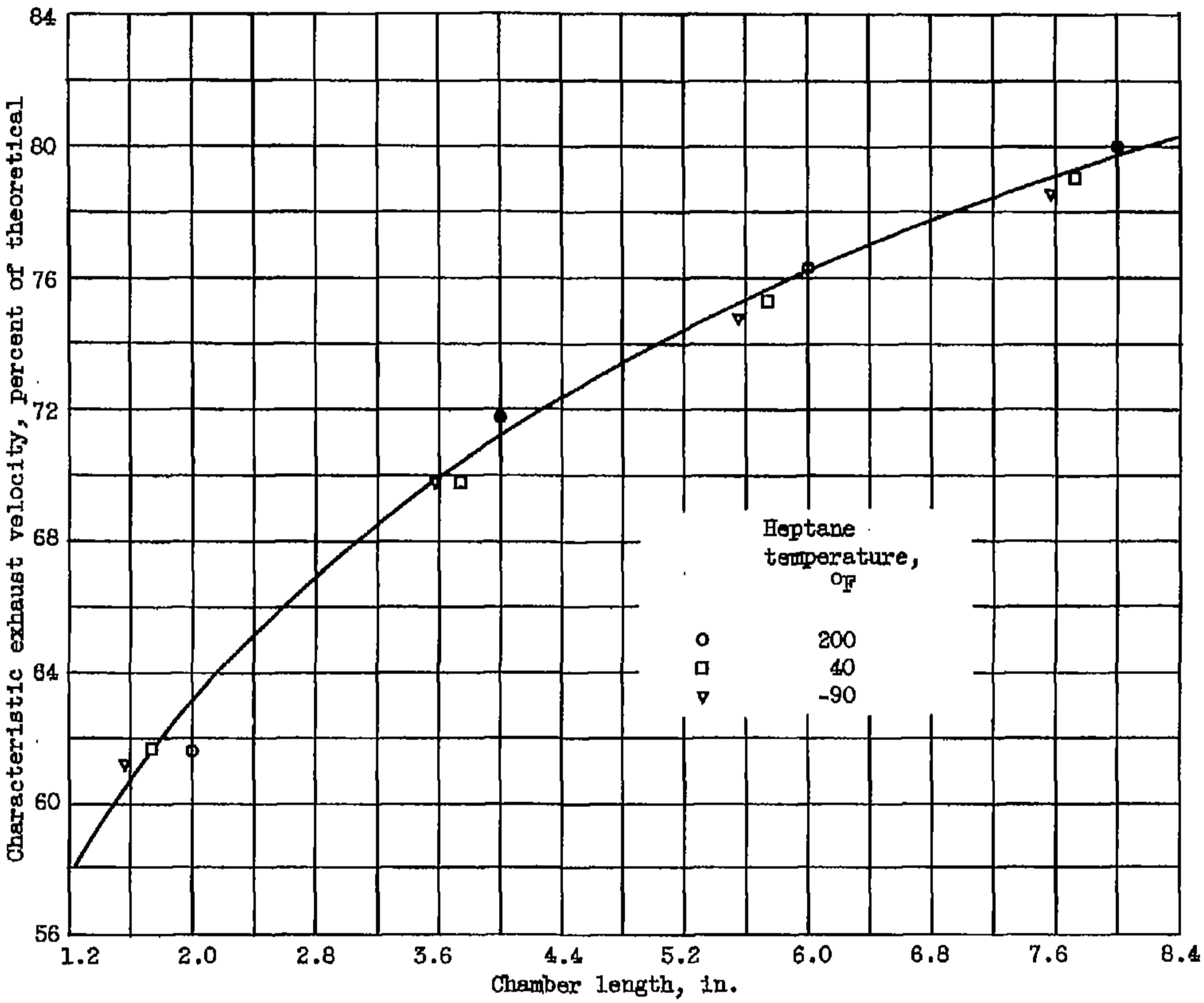

Figure 7. - Correlation of experimental data assuming equal increases in characteristic velocity from a 100° F increase in fuel temperature and a 0.14-inch increase in chamber length.

[redacted]

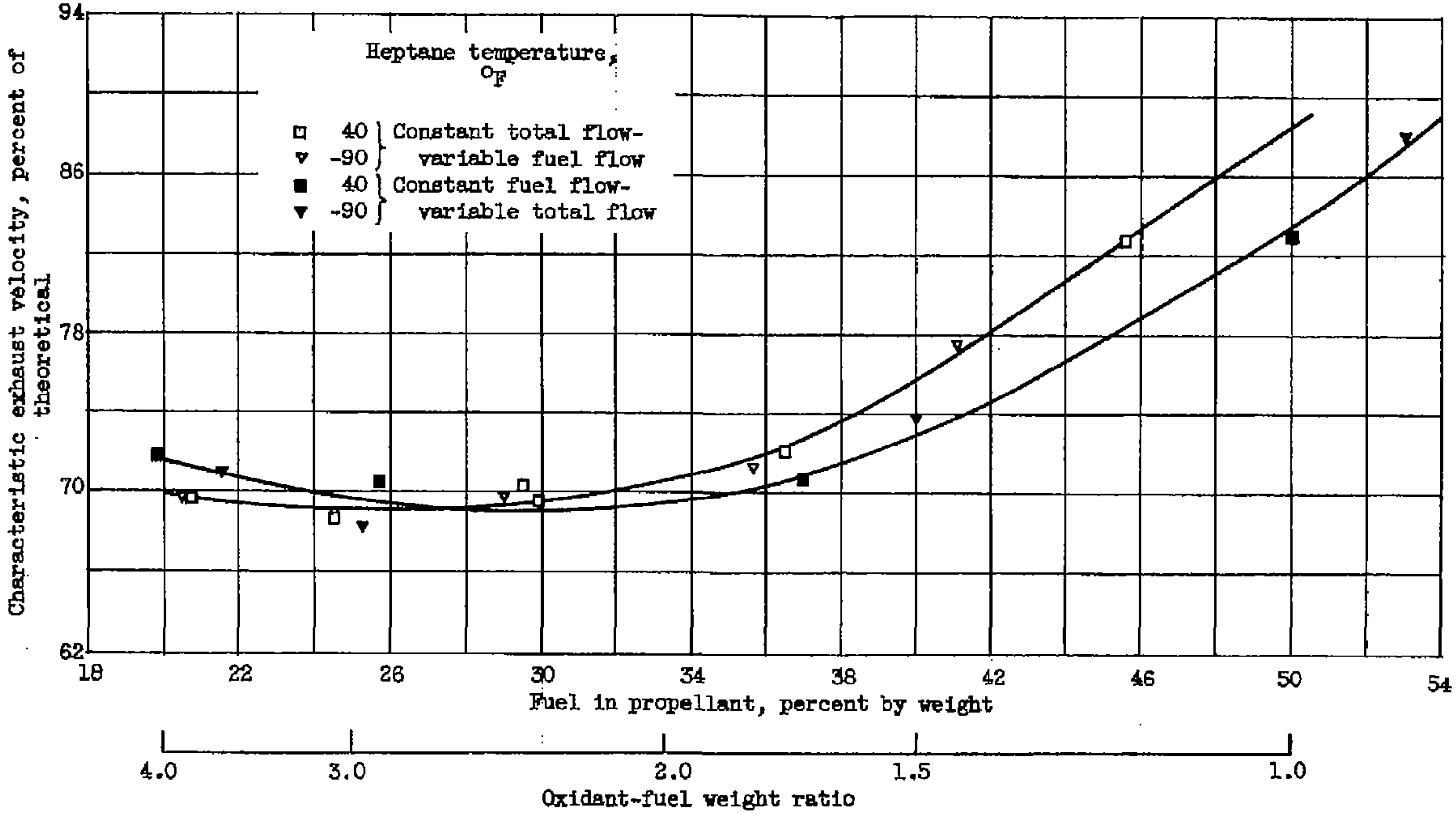

(a) Effect of mixture.

Figure 8. - Effect of mixture and fuel flow rate on characteristic exhaust velocity in a 4-inch chamber length.

[redacted]

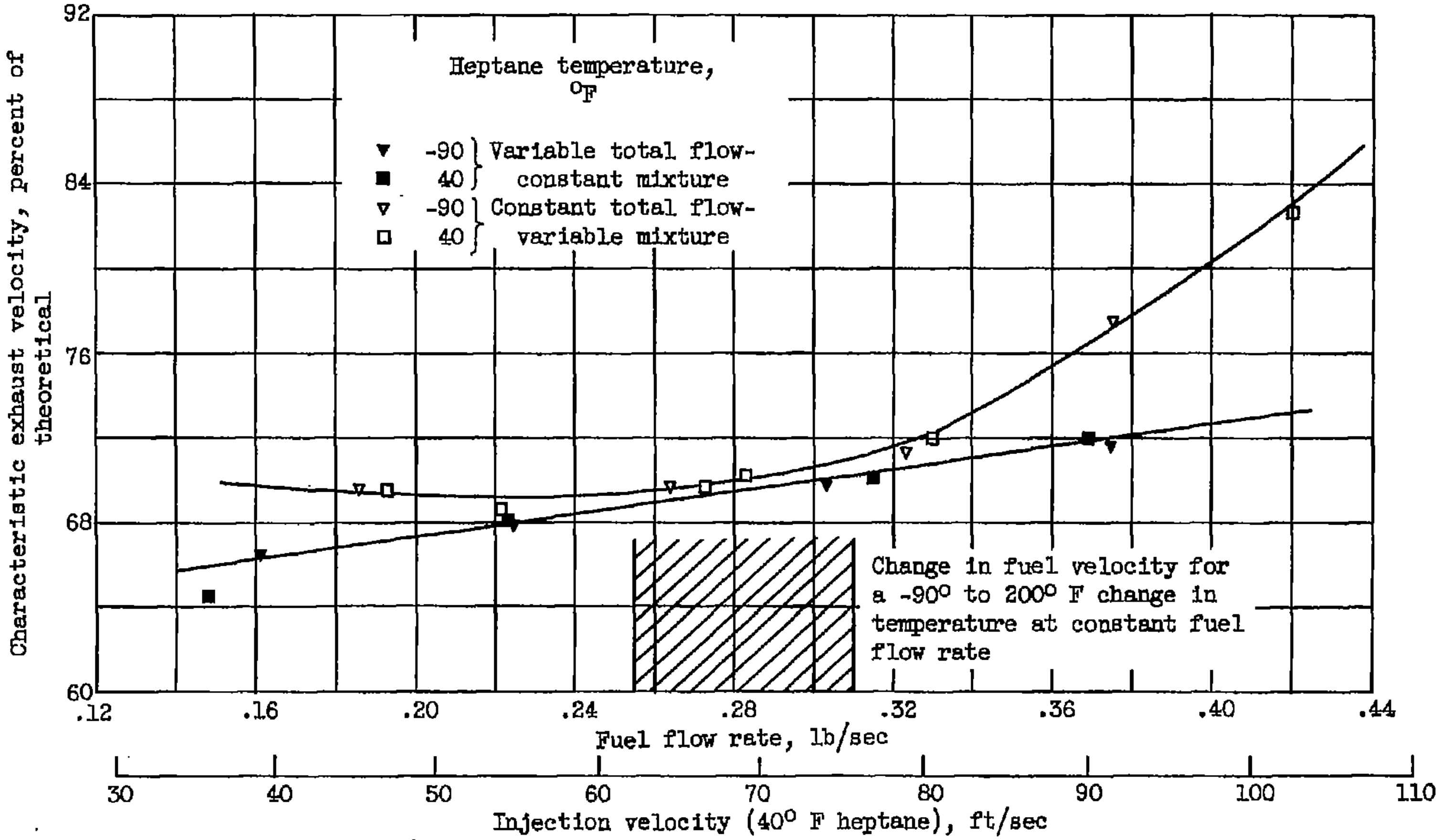

(b) Effect of fuel flow rate.

Figure 8. - Concluded. Effect of mixture and fuel flow rate on characteristic exhaust velocity in a 4-inch chamber length.